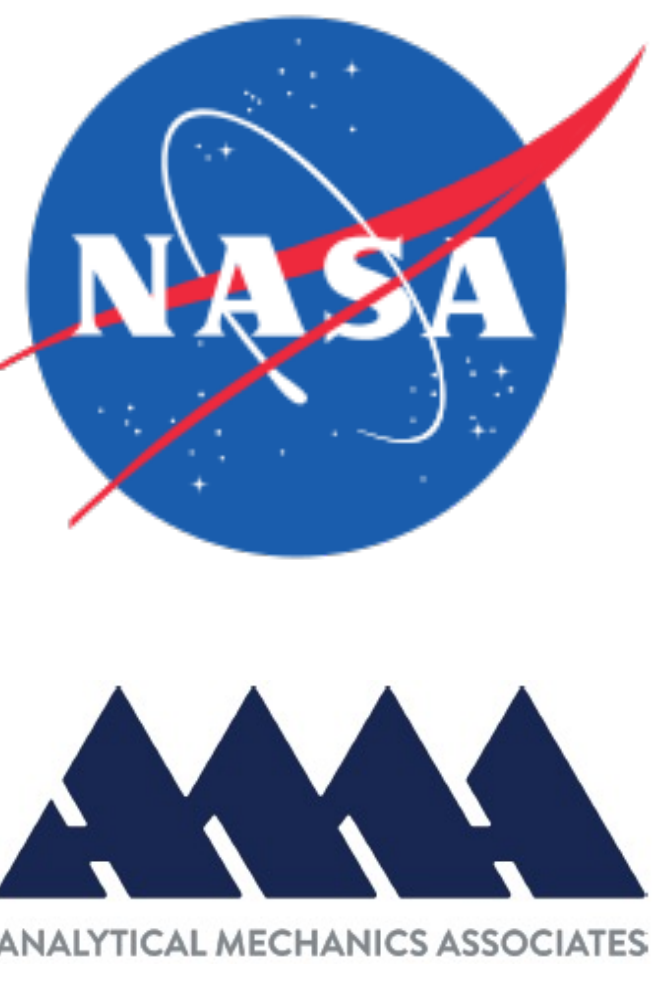


# Analysis of MSL/MEDLI Entry Data with Coupled CFD and Material Response

John M. Thornton<sup>1</sup>, Jeremie B.E. Meurisse<sup>1</sup>, Dinesh K. Prabhu<sup>1</sup>,  
Arnaud P. Borner<sup>1</sup>, Joshua D. Monk<sup>2</sup>, Nagi N. Mansour<sup>1</sup>, Brett A. Cruden<sup>1</sup>  
Analytical Mechanics Associates, Inc. at NASA Ames Research Center<sup>1</sup>, NASA Ames Research Center<sup>2</sup>



## Objective

The objective of this work is to showcase and analyze the coupling between the material response and the aerothermal environment in simulating the Mars atmospheric entry of the Mars Science Laboratory (MSL). In preparation for Mars 2020 post-flight analysis, the predictive material response capability is benchmarked against flight data from MSL. This work represents an important milestone toward the development of validated predictive capabilities for designing thermal protection systems for planetary probes.

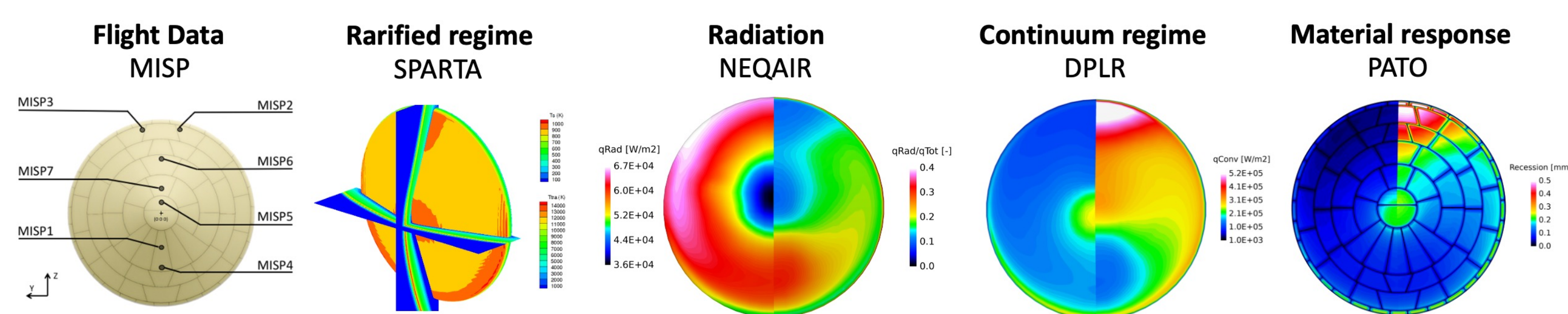


Fig. 1 Diagram showing the location of the MISP plugs on the MSL heatshield and highlighting the codes used in this study. The MISP plugs contained thermocouples at varying depths to provide in-depth temperature data during the MSL entry.

## Coupling Process

As shown in Figure 2, the workflow is divided into the following steps:

1. The aerothermal properties are computed in the Data Parallel Line Relaxation (DPLR) code [1] and used with the Nonequilibrium air radiation (NEQAIR) program [2] to compute radiative heating.
2. The thermal response inside the material is computed with the Porous material Analysis Toolbox based on Open-FOAM (PATO) [3,4,5] using a fixed blowing correction parameter  $\lambda$ .
3. The pyrolysis gases computed with PATO are used as inputs to a blowing boundary condition within DPLR.
4. The new environment properties from DPLR are used in NEQAIR to provide an updated solution
5. Both the updated aerothermal environment and radiative heating are used in PATO without blowing correction.
6. Steps 3-5 are then repeated until convergence in surface temperature is obtained.

Convergence in the radiative heating is generally achieved before surface temperature, at which point the radiative heating is no longer updated. Char mass loss rates are forced to zero to produce a non-receding surface condition.

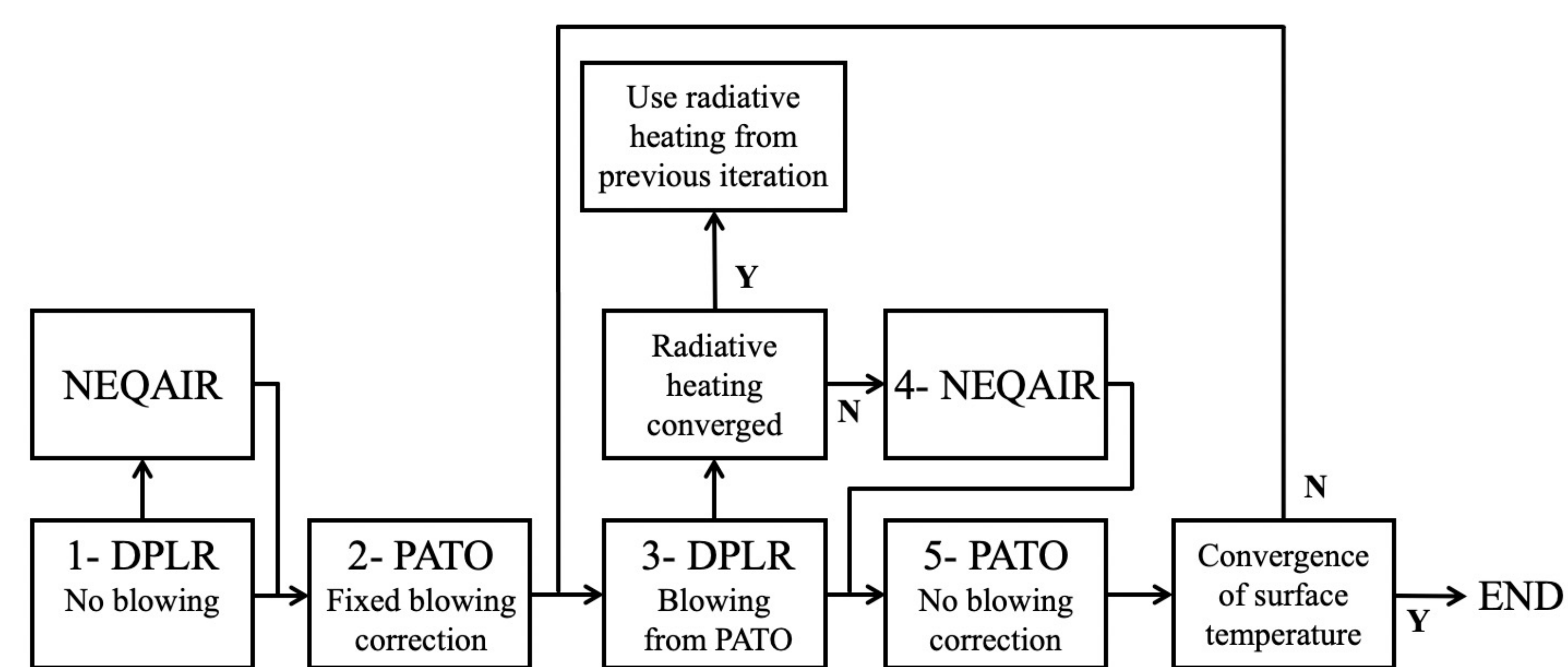


Fig. 2 Diagram showing the coupling process. DPLR and NEQAIR provide inputs to PATO which is initially run with a fixed blowing correction parameter  $\lambda$ . The blowing rates and species computed by PATO are then used as inputs to DPLR in a blowing boundary condition. Aerothermal environment (DPLR), radiative heating (NEQAIR), and material response (PATO) computations are then iterated without blowing corrections.

## Aerothermal Environment

### Rarefied Regime (SPARTA)

- DSMC simulations from SPARTA [6] produced environments up to 35s after the entry interface due to rarefied flow around the aeroshell early in the trajectory
- These environments are not iterated through the coupling process and use a fixed blowing correction parameter
- Radiative heating is assumed to be negligible and is not computed at early time points

### Continuum Regime (DPLR and NEQAIR)

- Chemical and thermal nonequilibrium
- 20 species model for Mars atmosphere in consideration of pyrolysis gases blown from material
- 177 lines of sight used with NEQAIR for radiative heating computations

## Material Response

The material response model in PATO is a mass and heat transfer model for porous reactive materials containing several solid phases and a single gas phase [4]. The following assumptions are made:

- Local thermal equilibrium at the pore scale
- B' boundary condition with tables for Mars entry
- Equilibrium chemistry

### Blowing Correction

The material response requires the pressure ( $p_w$ ) and heat transfer coefficient ( $C_H$ ) at the heatshield surface along with the enthalpy at the boundary layer edge ( $h_e$ ) which are given by DPLR. The blowing correction for the initial iteration is applied in the following way:

$$C'_H = C_H \frac{\ln\{1 + 2\lambda(B'_{pyro} + B'_{char})\}}{2\lambda(B'_{pyro} + B'_{char})}$$

$C'_H$	modified heat transfer coefficient
$\lambda$	blowing correction parameter
$B'_{pyro}$	nondimensional pyrolysis gas blowing rate
$B'_{char}$	nondimensional char blowing rate (zero in this study)

## Results

The coupling process has been performed up to 65s after the entry interface with ongoing work to continue marching in time. Differences in the temperature at the heatshield surface between the coupled and uncoupled simulations are significant and it is expected that these differences will increase as we approach peak heating.

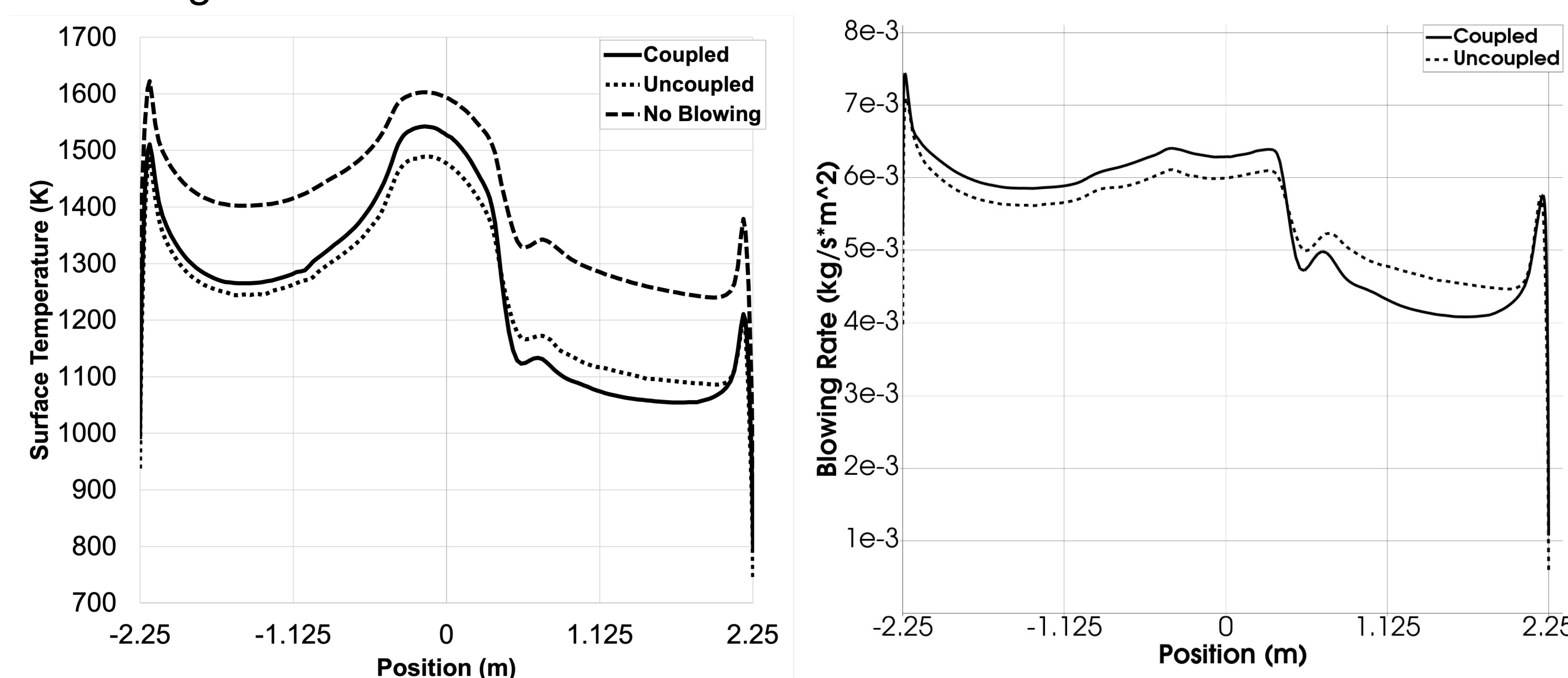


Fig. 3 Centerline plots of temperature (left) and blowing rate (right) at 65s at the heatshield surface.

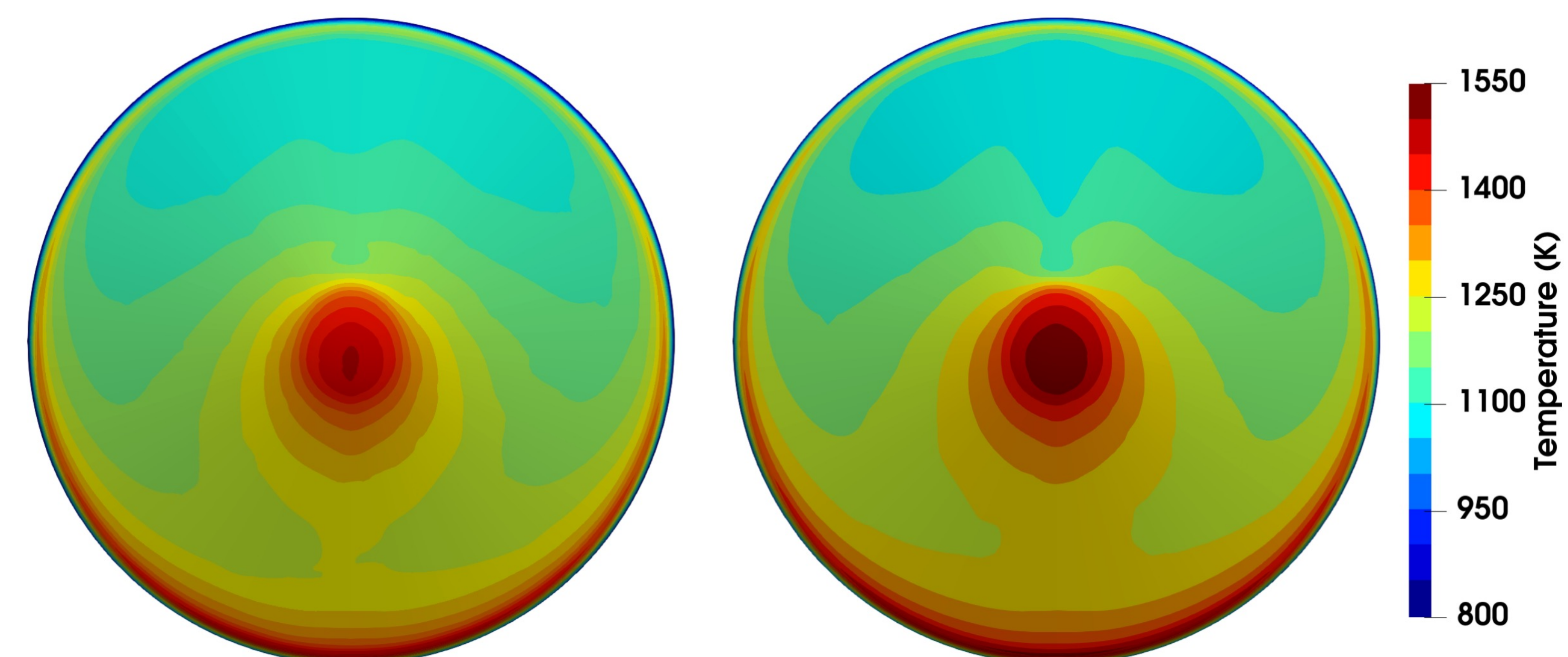


Fig. 4 Uncoupled (left) and coupled (right) surface temperatures at 65s.

## References

- [1] M.J. Wright et al. (2009), DPLR Code User Manual: Acadia-Version 4.01.1.
- [2] E. Whiting et al. (1996) NASA RP-1389.
- [3] J. Lachaud et al. (2014), J Thermophys Heat Tran, 28, 191–202.
- [4] J. Lachaud et al. (2017), Int J Heat Mass Tran, 108, 1406–1417.
- [5] J. B.E. Meurisse et al. (2018), Aerosp Sci Technol, 76, 497-511.
- [6] S.J. Plimpton et al. (2019), Phys. Fluids, 31(8), 086101.